[13] H. J. Buschmann, E. Cleve, E. Schollmeyer, *Inorg. Chim. Acta* **1992**, *193*, 93 – 97.
[14] C. Meschke, H. J. Buschmann, E. Schollmeyer, *Polymer* **1998**, *40*, 945 – 949.
[15] E. Lee, J. Heo, K. Kim, *Angew. Chem.* **2000**, *112*, 2811 – 2813; *Angew. Chem. Int. Ed.* **2000**, *39*, 2699 – 2701.
[16] S. G. Roh, K. M. Park, G. J. Park, S. Sakamoto, K. Yamaguchi, K. Kim, *Angew. Chem.* **1999**, *111*, 671 – 675; *Angew. Chem. Int. Ed.* **1999**, *38*, 637 – 641.
[17] H. J. Buschmann, K. Jansen, E. Schollmeyer, *J. Inclusion Phenom. Macrocyclic Chem.* **2000**, *37*, 231 – 236.
[18] B. D. Wagner, A. I. MacRae, *J. Phys. Chem. B* **1999**, *103*, 10114 – 10119.
[19] J. Kim, I. S. Jung, S. Y. Kim, E. Lee, J. K. Kang, S. Sakamoto, K. Yamaguchi, K. Kim, *J. Am. Chem. Soc.* **2000**, *122*, 540 – 541.
[20] A. Flinn, G. C. Hough, J. F. Stoddart, D. J. Williams, *Angew. Chem.* **1992**, *104*, 1550 – 1551; *Angew. Chem. Int. Ed. Engl.* **1992**, *31*, 1475 – 1477.
[21] W. L. Mock, N. Y. Shih, *J. Am. Chem. Soc.* **1989**, *111*, 2697 – 2699.
[22] W. L. Mock, N. Y. Shih, *J. Org. Chem.* **1986**, *51*, 4440 – 4446.
[23] P. Franchi, M. Lucarini, G. F. Pedulli, D. Sciotto, *Angew. Chem.* **2000**, *112*, 269 – 272; *Angew. Chem. Int. Ed.* **2000**, *39*, 263 – 266.
[24] Y.-S. Byun, O. Vadhat, M. T. Blanda, C. B. Knobler, D. J. Cram, *J. Chem. Soc. Chem. Commun.* **1995**, 1825 – 1827.
[25] C. Sheu, K. N. Houk, *J. Am. Chem. Soc.* **1996**, *118*, 8056 – 8070.
[26] P. D. Kirchhoff, M. B. Bass, B. A. Hanks, J. M. Briggs, A. Collet, J. A. McCammon, *J. Am. Chem. Soc.* **1996**, *118*, 3237 – 3246.
[27] K. N. Houk, K. Nakamura, C. Sheu, A. E. Keating, *Science* **1996**, *273*, 627 – 629.
[28] J. Yoon, D. J. Cram, *Chem. Commun.* **1997**, 1505 – 1506.
[29] R. C. Helgeson, C. B. Knobler, D. J. Cram, *J. Am. Chem. Soc.* **1997**, *119*, 3229 – 3244.
[30] D. J. Cram, M. T. Blanda, K. Paek, C. B. Knobler, *J. Am. Chem. Soc.* **1992**, *114*, 7765 – 7773.
[31] G. Girault-Vexlearschi, *Bull. Soc. Chim. Fr.* **1956**, 577 – 613.
[32] J. Rao, I. J. Colton, G. M. Whitesides, *J. Am. Chem. Soc.* **1997**, *119*, 9336 – 9340.
[33] W. Herrmann, B. Keller, G. Wenz, *Macromolecules* **1997**, *30*, 4966 – 4972.
[34] S. Chiu, S. J. Rowan, S. J. Cantrill, P. T. Glink, R. L. Garrell, J. F. Stoddart, *Org. Lett.* **2000**, *2*, 3631 – 3634.
[35] M. Ghosh, R. Zhang, R. G. Lawler, C. T. Seto, *J. Org. Chem.* **2000**, *65*, 735 – 741.
[36] Calculations were carried out with HyperChem 6.0, Hypercube Inc., with the implemented MM+ forcefield and parameter set for conditions in vacuo. The starting geometries of the inclusion complexes were optimized with a conformational search using AM1-calculated atomic charges. In the molecular dynamics runs, the egression from the optimized complexes was examined assuming a microscopic reversibility for the ingression process. At a constant simulation temperature of 398 K, which was required to observe the reaction within an acceptable simulation time, a bath relaxation time of 0.1 ps, and a 1 fs step size, the process was completed within a run time of 2 ps. The tendency of the ammonium group to remain bound to the carbonyl rim is exaggerated in the gas-phase calculations. However, the binding constants of the association complexes are significant in aqueous solution (see also ref. [37]), which indicates that solvation effects do not entirely offset this tendency.
[37] R. Hoffmann, W. Knoche, C. Fenn, H. J. Buschmann, *J. Chem. Soc. Faraday Trans.* **1994**, *90*, 1507 – 1511.
[38] G. W. Liesegang, M. M. Farrow, F. A. Vazquez, N. Purdie, E. M. Eyring, *J. Am. Chem. Soc.* **1977**, *99*, 3240 – 3243.
[39] J. Rebek, Jr., S. V. Luis, L. R. Marshall, *J. Am. Chem. Soc.* **1986**, *108*, 5011 – 5012.
[40] G. Wenz, *Clin. Drug Invest.* **2000**, *19*, 21 – 25.
[41] T. Haino, D. M. Rudkevich, J. Rebek, Jr., *J. Am. Chem. Soc.* **1999**, *121*, 11253 – 11254.
[42] SwaN-MR 3.2.0, Menarini Ricerche S.p.A, Florence (Italy).
[43] H. Mauser, *Formale Kinetik*, Bertelsmann Universitätsverlag, Düsseldorf, **1974**.

Combinatorial Discovery of New Photocatalysts for Water Purification with Visible Light**

Christian Lettmann, Heike Hinrichs, and Wilhelm F. Maier*

Photocatalytic conversion of air and water pollutants belongs to the most promising methods of environmental protection. Irradiation of a semiconducting oxide (SCO) with light of energy equal to or larger than the bandgap energy leads to the generation of electron – hole pairs, which can subsequently induce redox reactions at the SCO surface. Heterogeneous photocatalysis is an environmentally friendly method for the detoxification of water and air by sunlight, by which organic pollutants are converted to CO_2, H_2O, and mineral acids. Recent reviews were published discussing the underlying mechanisms and summarizing the state of the art.[1, 2] Research has been concentrated on anatase (TiO_2), which is photostable, nontoxic, cheap, and active. Due to its large bandgap of 3.2 eV, UV light ($\lambda < 400$ nm) is necessary to generate the electron – hole pairs. This is a major drawback for an efficient water detoxification with TiO_2, since only 3 % of the solar spectrum has wavelengths shorter than 400 nm.

We have discovered recently, that a variety of dopants in sol – gel derived TiO_2, such as Pt, Ir, and even coke, provide photocatalytic activity with visible light at wavelengths > 400 nm.[3, 6, 7, 12] These discoveries have convinced us, that there may be more photocatalytically active materials than presently known, and we have developed a combinatorial high-throughput technique in order to search more effectively for promising novel compositions. In recent years the potential power of combinatorial approaches and high-throughput (HT) screening for materials and catalysts has already been amply demonstrated,[4] while reports on the discovery of superior novel substances are still limited.

The aim of this work was to develop a reliable HT technique for the efficient discovery of new photocatalysts, capable of photodegrading water pollutants with visible light ($\lambda > 400$ nm). Due to their well-known photocatalytic properties, doped titanium oxides were selected as reference materials during the development of the method. Since nothing is known about the photocatalytic properties of the doped SCOs WO_3 or SnO_2 with visible light, these oxides have been selected as base materials for the discovery libraries.

The "library design" chosen consists of 45 transparent HPLC glass flasks (2 mL) arranged in an addressable rack of nine rows and five columns. The potential catalysts were

[*] Prof. Dr. W. F. Maier
Technische Chemie
Universität des Saarlandes
66123 Saarbrücken (Germany)
Fax: (+49) 681-302-2343
E-mail: w.f.maier@mx.uni-saarland.de
Dr. C. Lettmann, H. Hinrichs
Max-Planck-Institut für Kohlenforschung
Kaiser-Wilhelm-Platz 1, 45470 Mülheim an der Ruhr (Germany)

[**] We thank H. Kisch (Universität Erlangen – Nürnberg, Germany) for valuable discussions and information.

  1433-7851/01/4017-3160 $ 17.50+.50/0

synthesized directly in the HPLC flasks by means of a synthesis robot (Tecan Miniprep 50). For synthesis, a simple sol–gel procedure [Eq. (1)] was applied, which has already been shown to provide excellent photocatalysts.[3]

$$x\,\mathrm{M(OR)}_m + y\,\mathrm{M'X}_{2n} + \mathrm{H_2O} \xrightarrow{\mathrm{H^+}} (\mathrm{MO}_{m/2})_x(\mathrm{M'O}_{n/2})_y + y\,2n\,\mathrm{HX} + xm\,\mathrm{ROH} \quad (1)$$

Here, M stands for the base oxide (Ti, W, Sn), M′ for the dopant, and X for monovalent anions. The recipes were optimized for robotic synthesis. During the whole preparation procedure the reaction mixtures were agitated by a microtiterplate–orbital shaker (Heidolph Titramax 100) to ensure rapid and complete mixing of the reagents. The sol compositions are given in Table 1. For TiO_2 and SnO_2, isopropanol solutions of the corresponding tetraisopropoxides were employed as precursors; for WO_3, a synthesis procedure reported by Reisfeld and co-workers[5] was slightly modified, namely, a solution of H_2WO_4 in water was employed, prepared directly before the synthesis by passing a Na_2WO_4 solution through an acidic ion exchanger (Dowex 50WX8-400). Doping by addition of 1 or 3 mol% metal salts (0.05 N solutions in isopropanol) to the sol was used to modify the light-absorbing properties of the SCOs. For TiO_2 and SnO_2, hydrochloric acid was added to catalyse the gelation. For Pb and Ag as dopants, nitric acid was added instead of hydrochloric acid to avoid precepitation of the corresponding metal chlorides. In the case of WO_3, there was no addition of acid. This approach to doping does not require additional preparation steps and provides a mixed oxide, in which the dopant is homogeneously distributed throughout the solid matrix of the material.

Table 1. Calcination temperature T of the gels, pipetted volumes V, and concentrations c of the precursor solutions.

SCO	V(*i*PrOH) [μL]	V(SCO) [μL]	c(SCO) [mol L^{-1}]	V(dopant) [μL] (c = 0.05 N)	V(HCl) [μL] (c = 12 N)	T [°C]
TiO_2	251.6	396.9	1.0	79.4	7.8	400
SnO_2	159.3	396.9	0.282	67.6	5.7	400
WO_3	600	396.9	0.5	40.4	–	400

After gelation, the libraries were aged at room temperature for two weeks and subsequently calcined at 400 °C for 3 h to yield the mixed oxides, which remained in the HPLC flasks and were used as obtained. To determine the activity of the catalysts for photodegradation of water pollutants upon irradiation with visible light, 4-chlorophenol (4-CP) was chosen as model pollutant. 1 mL of a 4-CP solution ($c = 2.5 \times 10^{-4}$ mol L^{-1}), previously saturated with air, was added to each HPLC flask containing a catalyst, and the whole library was then subjected to irradiation with visible light. The light was provided by eight conventional fluorescence lamps (Osram Dulux S G23, 11 W; Figure 1 A), which emit light of wavelengths >400 nm. The lamps were mounted symmetrically side by side in order to assure homogeneous light intensity. A potassium chromate solution ($c = 1$ mol L^{-1}) was placed in a frosted-glass bath (solution depth ~1 cm) to remove remaining traces of UV light and to improve the homogeneity of the light-intensity distribution due to multiple scattering (Figure 1 B). The filter was positioned under the lamps, directly above the array of HPLC flasks containing the potential catalysts with aqueous pollutant solutions. The center of the flask array was aligned with the center of the lamp arrangement. The 5 × 9-library of HPLC flasks was illuminated for 2.5 h in the setup shown in Figure 1. During the whole experiment the library was agitated at the maximum shaker speed. After irradiation, the whole library was centrifuged at 4000 min^{-1} to ensure particle-free solutions. The solutions were analysed semi-automatically by HPLC using a standard HPLC sampling robot to quantify the 4-CP conversion.

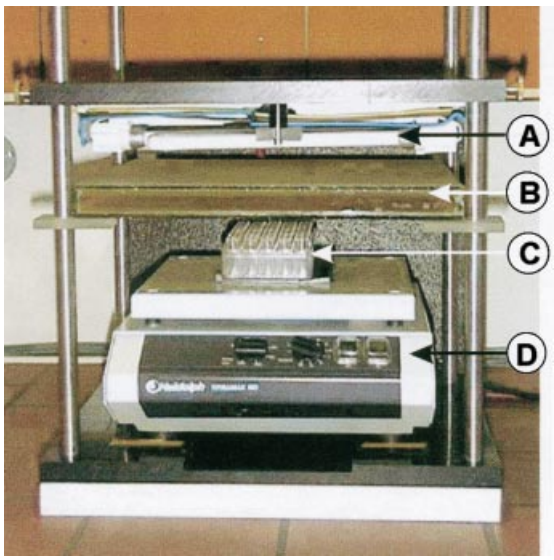

Figure 1. Front view of the experimental setup for visible-light irradiation of the libraries. A) Array of lamps (Osram Dulux S G 23, 11 W); B) bath of frosted glass filled with 1 M K_2CrO_4 solution; C) library of 45 HPLC flasks arranged in five columns and nine rows; D) orbital shaker (Heidolph Titramax 100).

The adsorption of 4-CP on the porous mixed oxides is a potential source of error. Adsorption experiments with the most active samples on the libraries confirmed that the decrease in solution concentration of 4-CP caused by adsorption at the catalyst surface remained below 5%. Therefore, only conversions >5% were associated with photocatalytic degradation. Clearly, the method does not yield identical solid catalysts with respect to particle size and mass-transport conditions. The gel catalysts on the flask bottom were used "as is" after the calcination; some remained clear gels, some showed severe cracks, others were powdery. Therefore the relative activity can be strongly affected by this state of the nature of the solid. This shortcoming was accepted, after we found that no false activities occured and that the clear as well as cracked gels exhibit photocatalytic activity. However, the relative activities detected in the high-throughput experiments should not be taken quantitatively.

TiO_2 library: In Figure 2 the results obtained from two TiO_2 libraries are summarized. As expected, no conversion was found with the undoped TiO_2 (position D5 and E10) confirming the absence of UV irradiation. For a few catalysts, high 4-CP conversions have been observed. Neglecting

  1433-7851/01/4017-3161 $ 17.50+.50/0

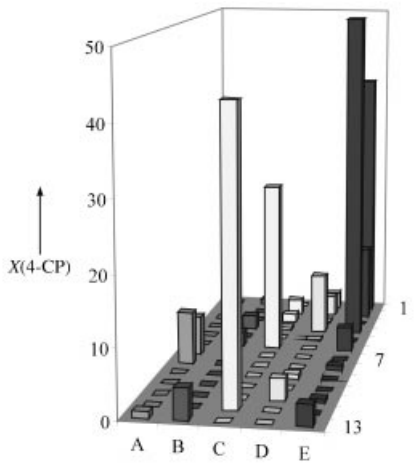

	A	B	C	D	E
1	$Sc(NO_3)_3 \cdot 5\,H_2O$	$V(acac)_3$	VO_2	$OV(OiPr)_3$	$CrCl_3 \cdot 6\,H_2O$
2	$MnCl_2$	$Mn(OAc)_3 \cdot 2\,H_2O$	$FeBr_2$	$FeCl_3 \cdot 6\,H_2O$	$Co(NO_3)_2 \cdot 6\,H_2O$
3	$Ni(OAc)_2 \cdot 4\,H_2O$	CuBr	$CuCl_2 \cdot 2\,H_2O$	$ZnCl_2$	$Y(NO_3)_3$
4	$Zr(OnPr)_4$	$NbBr_5$	MoO_2Cl_2	$RuCl_3$	$RhCl_3$
5	$PdCl_2$	$La(NO_3)_3 \cdot H_2O$	$HfCl_4$	undoped	WCl_4
6	WCl_6	$ReCl_5$	$IrCl_3$	$AuBr_3$	$Ce(NO_3)_3$
7	$PrCl_3 \cdot 6\,H_2O$	$NdCl_3 \cdot 6\,H_2O$	$SmCl_3$	$Eu(NO_3)_3 \cdot 6\,H_2O$	$Gd(NO_3)_3$
8	$TbCl_3 \cdot 6\,H_2O$	$DyCl_3 \cdot 6\,H_2O$	$HoCl_3 \cdot 6\,H_2O$	$Er(NO_3)_3 \cdot 5\,H_2O$	$TmCl_3 \cdot 6\,H_2O$
9	$Yb(NO_3)_3 \cdot 6\,H_2O$	$LuCl_3 \cdot 6\,H_2O$	$Ge(OEt)_4$	$In(NO_3)_3 \cdot H_2O$	$SnCl_2$
10	$SnCl_4$	BiI_3	$Ga(NO_3)_3 \cdot 9\,H_2O$	$Th(NO_3)_4 \cdot 5\,H_2O$	undoped
11	$BeCl_2$	$MgCl_2$	$CaCl_2$	$SrBr_2 \cdot 6\,H_2O$	$B(OH)_3$
12	$Al(NO_3)_3 \cdot 9\,H_2O$	$Si(OEt)_4$	$Na_2[PtCl_6] \cdot 6\,H_2O$	H_2SeO_3	$TeCl_4$
13	$LiNO_3$	$NaClO_4$	KOAc	Rb(acac)	$(NH_4)_2$-$Ce(NO_3)_6$

Figure 2. 4-CP conversions X for TiO_2-based mixed oxides after 2.5 h of irradiation. Each library member is identified by its position in the library, given by a column (A – E) and a row (1 – 13). The table contains the doping salts (1 mol % with respect to TiO_2) added to the corresponding positions during the sol – gel preparation. The library members showing 4-CP conversions $>5\,\%$ are shaded grey in the table; acac = acetylacetone.

conversions less than 5 %, the following dopands resulted in activation of the TiO_2 matrix: $RhCl_3$, $Na_2[PtCl_6] \cdot 6\,H_2O$, $CrCl_3 \cdot 6\,H_2O$, $IrCl_3$, $Co(NO_3)_2 \cdot 6\,H_2O$, $RuCl_3$, $TbCl_3 \cdot 6\,H_2O$, $MnCl_2$, $PrCl_3$. The photosensitisation of TiO_2 by $RhCl_3$, $Na_2[PtCl_6] \cdot 6\,H_2O$, and $IrCl_3$ has already been reported.[6] The activity of these materials with visible light was discovered by conventional experiments and especially the $Na_2[PtCl_6] \cdot 6\,H_2O$-doped TiO_2 was characterized in detail.[7] The same applies for the Cr- and Co-containing materials.[8, 9] The excellent agreement between our combinatorial with the conventional findings confirms the reliability and reproducibility of the high-throughput method developed. The positive effects of Tb, Mn, and Pr has not been reported in the literature and can be considered new discoveries. These materials are currently under investigation. Especially the activity of the Mn-doped material is of interest, since manganese oxide is cheap and nontoxic.

SnO_2 library: The $\sim$3.88 eV bandgap of SnO_2[10] corresponds to an excitation wavelength of 326 nm. This readily explains why the undoped SnO_2 (position E14) is not active under the experimental conditions chosen. Doping of SnO_2 drastically changes the situation (Figure 3): 22 out of the 71 library materials (two arrays) exhibit 4-CP conversions higher than 5 % upon visible-light irradiation. As with TiO_2, the Cr-, Mn-, Ru-, Ir-, and Pr-containing samples are active. In contrast to TiO_2, some other dopands also show beneficial effects: transition metals (Hf, V, Ta, Re, Au), lanthanoids (Ce, Tb, Ho), and even main-group metals (Bi, Ca). The origin of

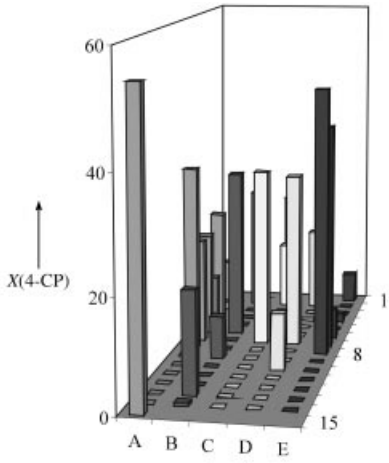

	A	B	C	D	E
1	$Sc(NO_3)_3 \cdot 5\,H_2O$	$Ti(OiPr)_4$	$V(acac)_3$	$OV(acac)_2$	$OV(O^iPr)_3$
2	$CrCl_3 \cdot 6\,H_2O$	$Cr(NO_3)_3 \cdot 9\,H_2O$	$MnCl_2$	$Mn(OAc)_3 \cdot 2\,H_2O$	$FeBr_2$
3	$FeCl_3 \cdot 6\,H_2O$	$Co(NO_3)_2 \cdot 6\,H_2O$	$Ni(OAc)_2 \cdot 4\,H_2O$	CuBr	$CuCl_2 \cdot 2\,H_2O$
4	$ZnCl_2$	$Y(NO_3)_3$	$Zr(OnPr)_4$	$NbBr_5$	MoO_2Cl_2
5	$RuCl_3$	$RhCl_3$	$PdCl_2$	$AgNO_3$	$La(NO_3)_3 \cdot H_2O$
6	$HfCl_4$	$Ta(OEt)_4$	WCl_4	WCl_6	$ReCl_5$
7	$IrCl_3$	$Na_2[PtCl_6] \cdot 6\,H_2O$	$AuBr_3$	$Ce(NO_3)_3$	$PrCl_3 \cdot 6\,H_2O$
8	$NdCl_3 \cdot 6\,H_2O$	$SmCl_3$	$Eu(NO_3)_3 \cdot 6\,H_2O$	$Gd(NO_3)_3$	$TbCl_3 \cdot 6\,H_2O$
9	$DyCl_3 \cdot 6\,H_2O$	$HoCl_3 \cdot 6\,H_2O$	$Er(NO_3)_3 \cdot 5\,H_2O$	$TmCl_3 \cdot 6\,H_2O$	$Yb(NO_3)_3 \cdot 6\,H_2O$
10	$LuCl_3 \cdot 6\,H_2O$	$BeCl_2$	$MgCl_2$	$CaCl_2$	$SrBr_2 \cdot 6\,H_2O$
11	$B(OH)_3$	$Al(NO_3)_3 \cdot 9\,H_2O$	$Ga(NO_3)_3 \cdot 9\,H_2O$	$In(NO_3)_3 \cdot H_2O$	$Si(OEt)_4$
12	$Ge(OEt)_4$	$SnCl_2$	$SnCl_4$	$PbClO_4 \cdot 3\,H_2O$	$SbCl_3$
13	$SbCl_5$	BiI_3	H_2SeO_3	$TeCl_4$	$Th(NO_3)_4 \cdot 5\,H_2O$
14	$LiNO_3$	$NaClO_4$	KOAc	Rb(acac)	undoped
15	$(NH_4)_2Ce(NO_3)_6$				

Figure 3. 4-CP conversions X for SnO_2-based mixed oxides after 2.5 h of irradiation. Each library member is identified by its position in the library, given by a column (A – E) and a row (1 – 15). The table contains the doping salts (1 mol % with respect to SnO_2) added to the corresponding positions during the sol – gel preparation. The library members showing 4-CP conversions $>5\,\%$ are shaded grey in the table.

  1433-7851/01/4017-3162 $ 17.50+.50/0

these activities is not understood yet. It is assumed that excitation of the dopant ions by visible light results in an excited state high enough in energy to allow transfer of the electron to the conductance band of SnO_2. None of these materials have been known for their photocatalytic properties.

WO_3 library: At 2.8 eV, the bandgap energy of WO_3 is much smaller than that of TiO_2 and SnO_2. As a consequence, only visible light of wavelengths $\lambda < 443$ nm is required to generate electron–hole pairs in undoped WO_3 and some activity could have been expected. However, as shown in Figure 4, the undoped WO_3 (position E14) and most other materials on the library are not active. This may be attributed to a high recombination rate of electron–hole pairs and/or the difficulty to photoreduce O_2.[11] Only very few dopants cause significant 4-CP conversion, among which Ir is by far the most active one, followed by Cr. Both materials have not been mentioned in the literature and are thus true discoveries.

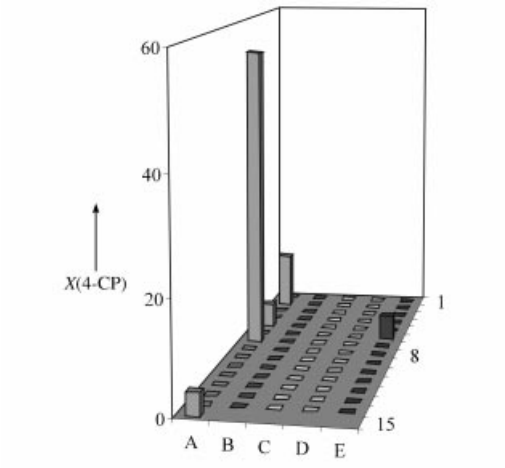

	A	B	C	D	E
1	$Sc(NO_3)_3 \cdot 5\,H_2O$	$Ti(OiPr)_4$	$V(acac)_3$	$OV(acac)_2$	$OV(OiPr)_3$
2	$CrCl_3 \cdot 6\,H_2O$	$Cr(NO_3)_3 \cdot 9\,H_2O$	$MnCl_2$	$Mn(OAc)_3 \cdot 2\,H_2O$	$FeBr_2$
3	$FeCl_3 \cdot 6\,H_2O$	$Co(NO_3)_2 \cdot 6\,H_2O$	$Ni(OAc)_2 \cdot 4\,H_2O$	CuBr	$CuCl_2 \cdot 2\,H_2O$
4	$ZnCl_2$	$Y(NO_3)_3$	$Zr(OnPr)_4$	$NbBr_5$	MoO_2Cl_2
5	$RuCl_3$	$RhCl_3$	$PdCl_2$	$AgNO_3$	$La(NO_3)_3 \cdot H_2O$
6	$HfCl_4$	$Ta(OEt)_4$	WCl_4	WCl_6	$ReCl_5$
7	$IrCl_3$	$Na_2[PtCl_6] \cdot 6\,H_2O$	$AuBr_3$	$Ce(NO_3)_3$	$PrCl_3 \cdot 6\,H_2O$
8	$NdCl_3 \cdot 6\,H_2O$	$SmCl_3$	$Eu(NO_3)_3 \cdot 6\,H_2O$	$Gd(NO_3)_3$	$TbCl_3 \cdot 6\,H_2O$
9	$DyCl_3 \cdot 6\,H_2O$	$HoCl_3 \cdot 6\,H_2O$	$Er(NO_3)_3 \cdot 5\,H_2O$	$TmCl_3 \cdot 6\,H_2O$	$Yb(NO_3)_3 \cdot 6\,H_2O$
10	$LuCl_3 \cdot 6\,H_2O$	$BeCl_2$	$MgCl_2$	$CaCl_2$	$SrBr_2 \cdot 6\,H_2O$
11	$B(OH)_3$	$Al(NO_3)_3 \cdot 9\,H_2O$	$Ga(NO_3)_3 \cdot 9\,H_2O$	$In(NO_3)_3 \cdot H_2O$	$Si(OEt)_4$
12	$Ge(OEt)_4$	$SnCl_2$	$SnCl_4$	$PbClO_4 \cdot 3\,H_2O$	$SbCl_3$
13	$SbCl_5$	BiI_3	H_2SeO_3	$TeCl_4$	$Th(NO_3)_4 \cdot 5\,H_2O$
14	$LiNO_3$	$NaClO_4$	KOAc	Rb(acac)	undoped
15	$(NH_4)_2Ce(NO_3)_6$				

Figure 4. 4-CP conversions X for WO_3-based mixed oxides after 2.5 h of irradiation. Each library member is identified by its position in the library, given by a column (A–E) and a row (1–15). The table contains the doping salts (1 mol% with respect to WO_3) added to the corresponding positions during the sol–gel preparation. The library members showing 4-CP conversions >5% are shaded grey in the table.

To confirm the photocatalytic properties of the newly discovered materials not based on TiO_2, a conventional study was added. The mixed oxides are abbreviated as with the amorphous mixed oxide (AM) notation AM-M′$_x$M, where M′ is the dopant and M is base oxide (AM-Ir$_1$W than stands for a mixed oxide composed of 1 mol% iridium oxide and 99 mol% tungsten oxide). The AM-Ir$_1$W and AM-Ce$_3$Sn mixed oxides were prepared on a 0.7 g scale by the sol–gel procedure, dried, calcined, and milled. The fine powders were used as photocatalysts in conventional experiments as described elsewhere.[12] 30 mg of the Sn- and 180 mg of the W-catalyst were dispensed in a 2.5×10^{-4} M aqueous solution of 4-CP in a stirred glass reactor, which was surrounded by a cooled, aqueous solution of K_2CrO_4 to absorb traces of extraneous UV radiation. The solution was irradiated for 100 min by seven fluorescence lamps (Osram Dulux S G23) and maintained at 25 °C. The decrease of 4-CP concentration was followed by HPLC analysis. In control experiments without UV radiation, a lack of photocatalytic activity was confirmed with commercial TiO_2 (Degussa P25). With AM-Pt$_2$Ti, a 30% conversion of 4-CP was obtained after 100 min, with AM-Ir$_1$W 8%, and with AM-Ce$_3$Sn 12%. Although the activities of the newly discovered SnO_2- and WO_3-based photocatalysts are still lower compared to the well-studied AM-Pt$_2$Ti, the photocatalytic activity of the new materials with visible light was confirmed under conventional reaction conditions. Both catalysts were characterized by various methods and compared to the undoped SnO_2 and WO_3, prepared by the same sol–gel procedure. Argon-adsorption isotherms showed these materials to be mesoporous (Brunauer–Emmett–Teller (BET) surface areas [$m^2 g^{-1}$] were 112/120 and 12/10 for the doped/undoped SnO_2 and WO_3, respectively). While the tin oxides are both X-ray amorphous, the tungsten oxides both show the diffraction pattern of small-particle WO_3. High-resolution transmission electron microscopy imaging revealed the presence of small (5 nm) SnO_2 crystallites embedded in the amorphous bulk matrix of the tin oxides, while the size ($\sim$10 nm) and number of the embedded crystallites in tungsten oxides are significantly larger. However, the microstructure of both photocatalysts is identical to that of the undoped, photocatalytically inactive reference oxides, which concludes that the photocatalytic activity of both materials can be attributed to dopant effects on the electronic structure of the bulk oxides.

The high-throughput method introduced here provides a low-cost, easy to handle, and powerful tool to screen for better photocatalysts. The reliability of the method was confirmed by the excellent agreement between the conventional and the high-throughput results found for Ti-based mixed oxides. Several new photocatalytically active materials based on doped TiO_2, SnO_2, and WO_3 were discovered. In few selected cases studied under conventional conditions their unusual photocatalytic activities were confirmed. This study shows that catalysts capable of utilising visible light can be discovered readily by the pragmatic use of a high-throughput technique. The overall activity of a photocatalyst is not only related to intrinsic electronic properties. Physicochemical

  1433-7851/01/4017-3163 $ 17.50+.50/0

characteristics are also of great importance, for example surface area, adsorption rate of pollutants and oxygen, concentration of surface hydroxyl groups, recombination rate of electron–hole pairs, crystallinity, and so forth. The complex nature of the origin of good photocatalytic properties in combination with our lack of knowledge related to the effects of oxide doping underlines the difficulty to predict the composition of the most active catalyst. The success of this simple study suggests that there may be many more photocatalytically active materials. It also indicates how little we know about the structure–activity relationship for visible-light photocatalysts.

Received: February 22, 2001 [Z16667]

[1] A. Mills, S. Le Hunte, *J. Photochem. Photobiol. A* **1997**, *108*, 1–35.
[2] D. Bahnemann in *The Handbook of Environmental Chemistry*, *Vol. 2*, *Part L* (Ed.: P. Boule), Springer, Berlin, **1999**, pp. 285–351.
[3] L. Zang, W. Macyk, C. Lange, W. F. Maier, C. Antonius, D. Meissner, H. Kisch, *Chem. Eur. J.* **2000**, *6*, 379–384.
[4] B. Jandeleit, D. J. Schaefer, T. S. Powers, H. W. Turner, W. H. Weinberg, *Angew. Chem.* **1999**, *111*, 2648–2689; *Angew. Chem. Int. Ed.* **1999**, *38*, 2494–2532.
[5] R. Reisfeld, M. Zayat, H. Minti, A. Zastrow, *Sol. Energy Mater.* **1998**, *54*, 109–120.
[6] H. Kisch, L. Zang, C. Lange, W. F. Maier, C. Antonius, D. Meissner, *Angew. Chem.* **1998**, *110*, 3201–3203; *Angew. Chem. Int. Ed.* **1998**, *37*, 3034–3036.
[7] L. Zang, C. Lange, I. Abraham, S. Storck, W. F. Maier, H. Kisch, *J. Phys. Chem. B* **1998**, *102*, 10765–10771.
[8] H. Yamashita, Y. Ichihashi, M. Takeuchi, S. Kishiguchi, M. Anpo, *J. Synchrotron Rad.* **1999**, *6*, 451–452.
[9] M. Iwasaki, M. Hara, H. Kawada, H. Tada, S. Ito, *J. Colloid Interface Sci.* **2000**, *224*, 202–204.
[10] H. Tada, A. Hattori, Y. Tokihisa, K. Imai, N. Tohge, S. Ito, *J. Phys. Chem. B* **2000**, *104*, 4585–4587.
[11] A. Sclafani, L. Palmisano, G. Marci, A. M. Venezia, *Sol. Energy Mater.* **1998**, *51*, 203–219.
[12] C. Lettmann, K. Hildenbrand, H. Kisch, W. Macyk, W. F. Maier, *Appl. Catal. B*, in print.

Rational Design of Low Molecular Mass Organogelators: Toward a Library of Functional *N*-Acyl-1,ω-Amino Acid Derivatives**

Gudrun Mieden-Gundert, Lars Klein, Marco Fischer, Fritz Vögtle,* Karine Heuzé, Jean-Luc Pozzo, Martine Vallier, and Frédéric Fages*

The gelation of organic fluids by low molecular mass organic gelators is a fascinating phenomenon in that it represents a spectacular macroscopic expression of molecular self-assembly.[1, 2] Organogels have especially attracted much interest as a unique class of nanostructured organic materials with far-reaching applications.[1–3] A major challenge that arises thus concerns the elaboration of novel design strategies enabling the synthesis of new series of gelator molecules. In that connection, structurally simple compounds,[4] easy to synthesize and available in large amount from cheap starting materials, are desirable from both fundamental and practical standpoints. Several design approaches have been already proven successful, that are based on the use of various self-recognition units.[5] Hydrogel formation with amphiphilic molecules was also reported recently.[6, 7]

Fatty acid compounds are known to form gelatinous and curd-fiber phases in organic solvents, but typically at high concentrations.[8] Within this series of amphiphile compounds, the behavior of 12-hydroxystearic acid (12-HSA, Scheme 1) attracted special attention.[9] Indeed, this compound displays a remarkably improved gelation ability in organic solvents as compared to analogous molecules lacking a hydrogen bonding group in the hydrophobic chains.[10] It occurred to us that *N*-acyl-1,ω-amino acid compounds presenting similar structural features to 12-HSA could also provide gelation ability,

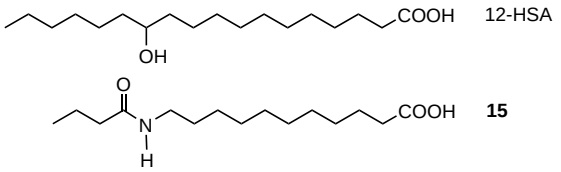

Scheme 1. Structure of 12-HSA in comparison with the new gelator **15**.

[*] Prof. Dr. F. Vögtle, G. Mieden-Gundert, Dr. L. Klein, Dr. M. Fischer
Kekulé-Institut für Organische Chemie und Biochemie
Gerhard-Domagk-Strasse 1, 53121 Bonn (Germany)
Fax: (+49) 228-73-56-62
E-mail: voegtle@uni-bonn.de
Prof. Dr. F. Fages, Dr. K. Heuzé, Dr. J.-L. Pozzo, Dr. M. Vallier
Group of Supramolecular Chemistry and Catalysis
UMR 5802, University Bordeaux 1
33405 Talence Cedex (France)
Fax: (+33) 556-84-6994
E-mail: f.fages@lcoo.u-bordeaux.fr

[**] We thank the CNRS, the University Bordeaux 1, La Région Aquitaine, and the Deutsche Forschungsgemeinschaft (DFG, Vo 145/49-1). This work was supported by COST Chemistry in the framework of COST D11 Action (network D11/0015/99).We are also grateful to Dr. Christoph Schalley for mass-spectroscopic characterizations.

  1433-7851/01/4017-3164 $ 17.50+.50/0